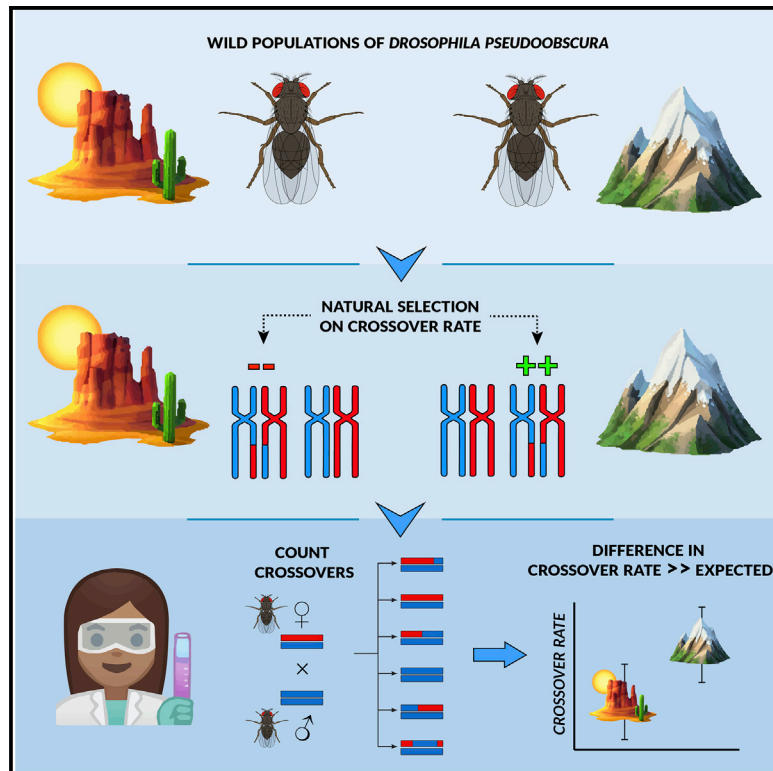


Current Biology

Natural Selection Shapes Variation in Genome-wide Recombination Rate in *Drosophila pseudoobscura*

Graphical Abstract



Authors

Kieran Samuk,
Brenda Manzano-Winkler,
Kathryn R. Ritz, Mohamed A.F. Noor

Correspondence

ksamuk@gmail.com

In Brief

Recombination rate has long been hypothesized to be subject to the forces of evolution. Studying wild populations of *Drosophila pseudoobscura*, Samuk et al. show that recombination rate exhibits abundant genetic variation and evidence of natural selection.

Highlights

- Recombination rate varies within and between natural populations of *D. pseudoobscura*
- Genetic variation for recombination rate manifests mainly at the genome-wide scale
- Interpopulation differences in recombination rate show evidence of natural selection

Natural Selection Shapes Variation in Genome-wide Recombination Rate in *Drosophila pseudoobscura*

Kieran Samuk,^{1,2,*} Brenda Manzano-Winkler,¹ Kathryn R. Ritz,¹ and Mohamed A.F. Noor¹

¹Department of Biology, Duke University, Durham, NC 27708, USA

²Lead Contact

*Correspondence: ksamuk@gmail.com

<https://doi.org/10.1016/j.cub.2020.03.053>

SUMMARY

While recombination is widely recognized to be a key modulator of numerous evolutionary phenomena, we have a poor understanding of how recombination rate itself varies and evolves within a species. Here, we performed a comprehensive study of recombination rate (rate of meiotic crossing over) in two natural populations of *Drosophila pseudoobscura* from Utah and Arizona, USA. We used an amplicon sequencing approach to obtain high-quality genotypes in approximately 8,000 individual backcrossed offspring (17 mapping populations with roughly 530 individuals each), for which we then quantified crossovers. Interestingly, variation in recombination rate within and between populations largely manifested as differences in genome-wide recombination rate rather than remodeling of the local recombination landscape. Comparing populations, we discovered individuals from the Utah population displayed on average 8% higher crossover rates than the Arizona population, a statistically significant difference. Using a Q_{ST} - F_{ST} analysis, we found that this difference in crossover rate was dramatically higher than expected under neutrality, indicating that this difference may have been driven by natural selection. Finally, using a combination of short- and long-read whole-genome sequencing, we found no significant association between crossover rate and structural variation at the 200–400 kb scale. Our results demonstrate that (1) there is abundant variation in genome-wide crossover rate in natural populations, (2) at the 200–400 kb scale, recombination rate appears to vary largely genome-wide, rather than in specific intervals, and (3) interpopulation differences in recombination rate may be the result of local adaptation.

INTRODUCTION

Meiotic recombination is the exchange of genetic material between homologous chromosomes that occurs during meiosis. This exchange has two major forms, crossing over and non-crossover gene conversion, both of which are initiated by the formation of a double-strand break during meiosis. Recombination,

particularly crossing over, is a key mediator of chromosome pairing during meiosis, with most species exhibiting an average of one crossover per chromosome arm [1, 2].

While physical constraints often set a lower bound on rates of recombination, the evolution of recombination rate and particularly the rate of crossing over (i.e., number of crossovers per generation in a genomic interval) can have far-reaching effects on nearly every evolutionary process [2–4]. For example, recombination rates can modulate processes as diverse as adaptation to a new environment, the evolution of reproductive isolation, and the dynamics of introgression between populations [5–8]. More generally, recombination rate determines the degree to which an individual's parental chromosomes are mixed in their gametes—i.e., how often novel allelic combinations are generated in their gametes. Increases or decreases in this rate can be favored under different evolutionary or ecological conditions. For example, increasing the rate of recombination can facilitate adaptation by increasing the probability that adaptive and maladaptive alleles will be decoupled or that adaptive alleles will be brought together in the same genotype (i.e., overcome Hill-Robertson interference [9]). Increased rates of recombination are similarly favored when fitness optima change rapidly between generations, e.g., under fluctuating selection [10]. On the other hand, lower recombination rates can be favored under scenarios in which adaptive combinations of alleles are at risk of being broken apart, such as under maladaptive gene flow [11]. Reduction/suppression also appears to have important consequences for the evolution of reproductive isolation [11, 12] and patterns of introgression and divergence in the genome [8, 13, 14].

While there is a rich theoretical literature focused on the evolution of recombination rate, empirical studies have lagged somewhat behind. One reason for this may be that recombination rate is difficult to quantify directly—it generally requires the construction of a linkage map from a genetic cross and/or cytological visualization of recombination-associated proteins [2, 15, 16]. Recently, many studies have attempted to overcome this difficulty by instead estimating a population genetic quantity known as ρ , the population scaled recombination rate [17]. This quantity is the product of four times the effective population size and realized recombination rate (sometimes denoted “c”) [18]. The general approach to estimating ρ is to perform coalescent simulations and fit a simulated value of ρ to observed patterns of linkage disequilibrium (LD) [19–21]. While this approach has proven successful at recapitulating many of the general features of the recombination landscape in many species, it is not able to disentangle changes in LD per se (e.g., as a result of selection or

demography) from changes in recombination rate (either locally or genome-wide) [21, 22]. Further, these methods are highly sensitive to increases in LD that occur as a result of gene flow between populations [22–24]. As such, LD-based methods are likely to be less appropriate for the study of the evolution of recombination rate than direct estimates of recombination rate.

In spite of methodological difficulties, there has been a recent resurgence of interest in the empirical study of the evolutionary causes and consequences of recombination rate [2, 4, 25]. One key contributor to this resurgence has been the democratization of high-throughput genotyping, which has increased the tractability of creating high-density linkage maps in non-model species (e.g., using pedigreed populations or gametic sequencing [26, 27]). The increased availability of such linkage maps has in turn led to a growing appreciation of the enormous diversity in recombination rate that exists between taxa [25]. This variation can manifest globally, i.e., genome-wide, or locally, i.e., along a specific tract of a chromosome [25, 28].

Studies using direct estimates of recombination rate have largely focused on describing differences in recombination between species or sexes [25, 29, 30]. However, there are surprisingly few studies focused on directly testing evolutionary hypotheses concerning variation in recombination rate. For example, a key question that emerges from the theoretical literature is, is variation in recombination rate shaped by natural selection [5, 10, 31]? While a tempting research direction, the difficulty in measuring and manipulating recombination rate makes testing adaptive hypothesis a non-trivial enterprise [2, 4]. One approach may be experimental evolution, in which the proposed selective agent that favors/disfavors changes in recombination rate is experimentally varied, evolved differences in recombination rate are quantified, and these differences are then compared to a null (non-adaptive) expectation [32]. This approach is powerful but highly laborious and difficult to apply to natural systems. A more broadly applicable method for detecting the influence of natural selection on a quantitative trait is perhaps the Q_{ST} - F_{ST} approach [33]. Originating in the quantitative genetics literature, this powerful method is designed to answer the question: are the observed differences between populations in a quantitative trait greater than expected on the basis of drift alone [33, 34]? This question is formalized as a statistical hypothesis test that compares variation in a quantitative trait (Q_{ST}) within and between populations to a null distribution of variation in neutral genetic markers (F_{ST}) within and between populations [34, 35]. While the Q_{ST} - F_{ST} is subject to many of the same limitations and assumptions as other methods for studying natural selection in the wild it is also has a number of advantages, including the ability to detect very recent natural selection and robustness to a variety of common demographic perturbations (e.g., changes in population size or levels of migration). While the Q_{ST} - F_{ST} method has enjoyed great success in the quantitative and evolutionary genetics literature, it has not yet been applied to testing the role of selection in shaping recombination rate. Given its flexibility and applicability to any quantitative trait, we see Q_{ST} - F_{ST} as an ideal approach to this problem.

Along with quantifying intraspecific variation and the role of natural selection, we also have a poor understanding of the genetic basis of differences in recombination rate between populations and species. As is the case for other traits, identifying the genetic architecture of evolutionary changes in recombination rate allows for a

more complete explanation for how and why recombination rate evolves [36]. One specific question is the degree to which variation in recombination rate manifests as a local versus global phenomenon. Local variation in recombination can arise due to structural variants that suppress recombination such as inversions and large deletions [37–39]. In contrast, global variation can arise from mutations in the genes involved in meiosis and/or double-strand break repair pathways [40]. Modifiers of both global and local rates of recombination have been identified in laboratory and/or interspecific crosses, but their occurrence in natural populations of individual species is only just beginning to be explored [26, 29, 40–42].

Here, we performed a comprehensive study of recombination rate (meiotic rates of crossover) in two natural populations of *Drosophila pseudoobscura* from Utah and Arizona, USA. We made use of modern sequencing and genetic map construction methods, along with the Q_{ST} - F_{ST} approach. We first constructed individual-level genetic maps and discovered ample quantitative genetic variation for recombination rate within and between populations of *D. pseudoobscura*. Interestingly, we found that this variation largely manifested as differences in genome-wide recombination rate rather than remodeling of the local recombination landscape. Interindividual differences in local genome structure (e.g., structural variation) did not appear to influence recombination rate at the scale of measurement, again suggesting that variation in recombination rate is largely governed by global modifiers. Finally, using the Q_{ST} - F_{ST} approach, we discovered that between-population differences in recombination rate are much greater than expected under a pure-drift model, suggesting that natural selection may have shaped recombination rate variation in *D. pseudoobscura*. Together, these results provide direct evidence for genetic variation in global modifiers of recombination and support the hypothesis that natural selection can and does act to shape recombination rate in natural populations.

RESULTS

Genome-wide Recombination Rate Varies within and between Populations

Genome-wide recombination rate varied significantly within and between the *D. pseudoobscura* populations we studied. Within lines, there was a range of 4.27–5.86 crossovers per genome, corresponding to 0.85–1.00 crossovers per chromosome arm on average (Figure 1A). This between-line variation was statistically significant ($p < 2.2 \times 10^{-16}$, likelihood ratio test statistic = 141.13, $df = 1$, comparison via dropping random effect of inbred line). At the population level, lines from American Fork Canyon, UT, had 5.20 ± 0.17 crossovers per genome on average, while lines from Madera Canyon, AZ, had 4.82 ± 0.21 crossovers per genome on average, a significant difference in genome-wide crossover rate (Figure 1B; type II Wald test, $p = 0.018$, $df = 1$; likelihood ratio test, $X^2_1 = 4.794$, $p = 0.028$).

That said, despite genome-wide differences, the local rates of recombination were extremely similar among individuals and populations (Figures 1C and 2A; $R^2 = 0.96$, correlation test $t = 68.866$, $df = 207$, $< 2.2 \times 10^{-16}$). Indeed, in contrast to the aggregate genome-wide difference we observed in Figure 1B, only 19 of the 209 recombination intervals we assayed displayed significant population-specific differences at the $\alpha = 0.05$ level, and none were significant after false discovery rate (FDR) correction

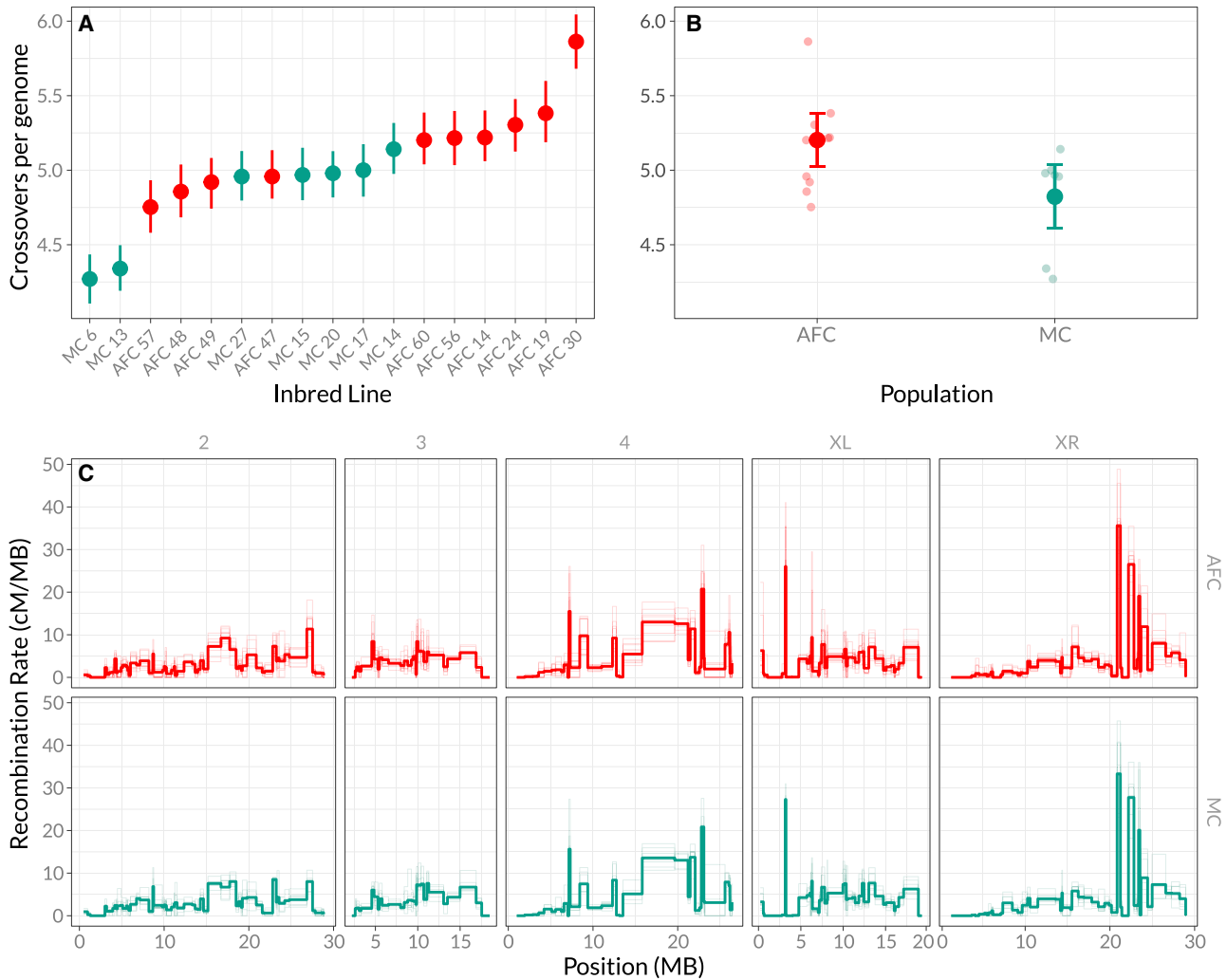


Figure 1. Recombination Rate Varies within and between Populations of *D. pseudoobscura*

(A) Variation in genome-wide crossing over frequency for 17 inbred lines. Lines are colored according to their population of origin (green, MC [Madera Canyon, AZ]; red, AFC [American Fork Canyon, UT]). Points depict the mean crossover frequency for each line with vertical lines representing 95% confidence intervals ($n = 384$ per line).

(B) Differences in crossover frequency between AFC and MC. Jittered points are individual line means (from A), and larger points are marginal means derived from mixed model regression coefficients along with 95% confidence intervals (error bars).

(C) Variation in recombination rate across the genome. Each panel depicts recombination rate along a single chromosome arm (columns) in one of two populations (rows). Thick lines depict population average recombination rates, with lighter lines depicting rates for individual inbred lines. Note that in *D. pseudoobscura* the X chromosome takes the place of a chromosome “1.”

See [Figure S2](#) for comparisons of marker orders between maps. See [Figure S3](#) for an example of GLMM model fit diagnostics. See [Figures S4](#) and [S5](#) for information on the fine-scale differences in recombination between populations and lines. See [Tables S1](#) and [S2](#) for raw crossover estimates.

([Figure S4](#)). That said, some recombination intervals did show a significant effect of inbred line identity ([Figure S5](#)) suggesting that there may be genetic variation for local recombination rates at the 200–400 kb scale. Finally, we found that chromosome-scale recombination rates were highly correlated *within* lines, such that there was a strong trend that lines with high recombination rate on one chromosome tended to also have high recombination on other chromosomes ([Figure 2B](#); average $R^2 = 0.78$, all correlations significant via correlation tests, $p < 0.0001$). In sum, these results suggest that phenotypic variation in recombination rate within and between populations largely manifests at the genome-wide scale. That said, our marker density prevents us from ruling out

finer-scale population-level differences in the recombination landscape (i.e., at the <200 kb scale).

Population Differences in Recombination Rate Are Greater Than Expected under Neutrality

As expected from previous studies, genetic divergence between Madera Canyon, AZ, and American Fork Canyon, UT, was very low: genome-wide Weir and Cockerham’s F_{ST} was approximately 0.0039 ([Figure 3A](#); mean F_{ST} of 6 591 high-quality SNPs, $MAF > 0.1$, $LD > 0.2$; F_{ST} computed using WGS from inbred lines was highly similar). Examining variation in recombination rate, we estimated a within-population (between line) variance component of

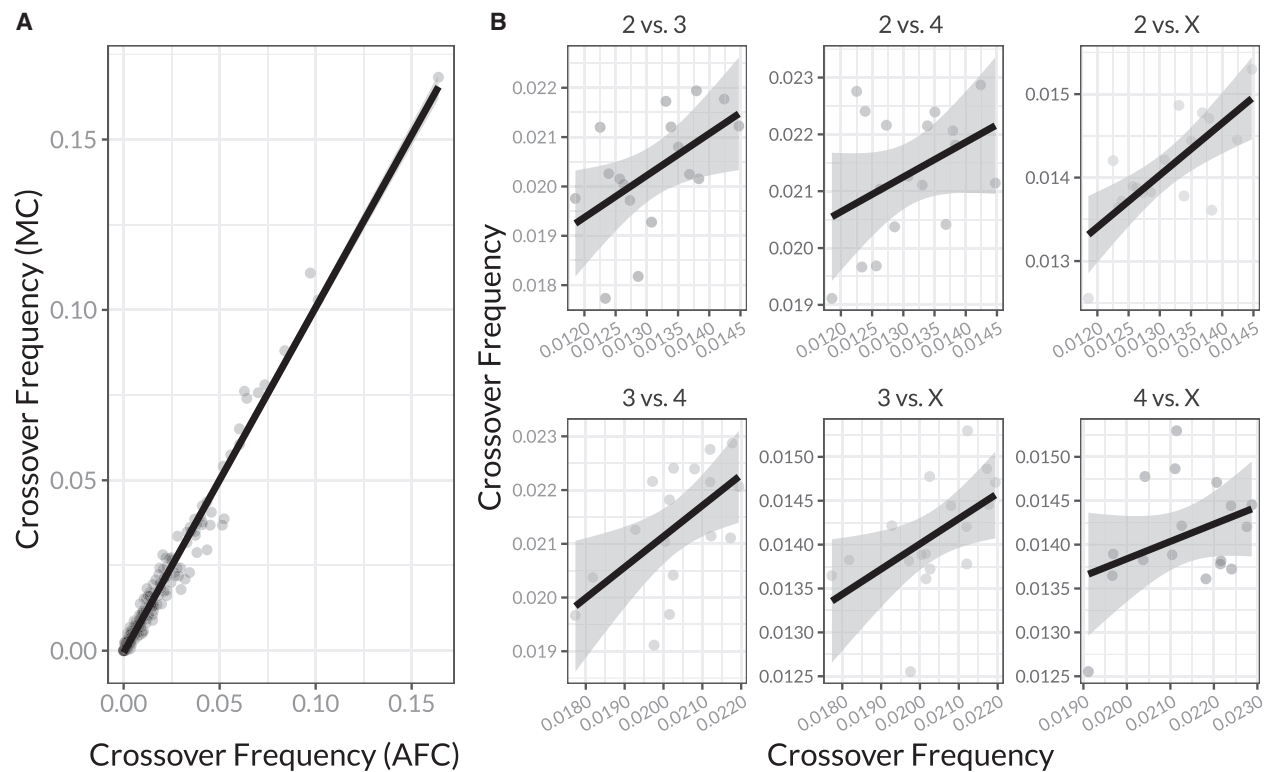


Figure 2. Recombination Rate Varies Primarily at the Genome-wide Scale

(A) The correlation between recombination rates measured in genomic windows (~300 kb in size) in the MC and AFC populations. Each dot depicts a single genomic window (all chromosomes combined).

(B) The correlation between chromosome-wide mean recombination rates between all pairs of chromosomes. Each point represents the recombination rate on two chromosomes for a single inbred line. Points and lines are colored to indicate the particular pair of chromosomes being compared. Positive trends indicate that recombination rates are consistent across chromosomes within lines (i.e., they vary genome-wide and not idiosyncratically across chromosomes).

See [Figure S2](#) for comparisons of marker orders and recombination fractions between line-specific genetic maps and [Figures S4](#) and [S5](#) for more detailed analyses of local variation in recombination rate.

0.066 and a between-population variance component of 0.018, yielding an observed Q_{ST} of 0.212 ([Figure 3A](#); dashed arrow). Our parametric bootstrap simulations of Q_{ST} suggest that this value of Q_{ST} is highly unlikely to be observed under neutrality (0 of 10,000 Q_{ST} replicates were greater than the observed value of Q_{ST} ; thus, $p < 1.0 \times 10^{-4}$). Similarly, the parametric bootstrap estimates of $Q_{ST}-F_{ST}$ under neutrality do not overlap with the parametric bootstrap observed values of $Q_{ST}-F_{ST}$, even when taking into account sampling variance ([Figure 3B](#)). Together, these results indicate that, while the observed phenotypic difference in recombination rate between Madera Canyon (MC) and American Fork Canyon (AFC) is modest, it greatly exceeds its expected value under neutrality. This result is consistent with the hypothesis that natural selection has driven the observed difference in recombination rates between populations.

Nonsynonymous Differences in Meiosis Genes Are Correlated with Recombination Rate

Of the 46 candidate genes examined, 33 had at least one nonsynonymous polymorphism. Of these 33 genes, there were a total of 357 codons (out of a total of 29,964) with at least one nonsynonymous polymorphism. After controlling for multiple comparisons three of these sites in two genes (*asp* and *mei-41*) were significantly

associated with crossover rate (FDR adjusted $p < 0.05$, [Figure 4A](#)). Both *asp* and *mei-41* play key roles in meiosis and recombination: *asp* is involved in spindle pole formation during cell division (both mitotic and meiotic) whereas *mei-41* (also known as ATR) is an important regulator of double-strand break repair and meiosis checkpoint activation [43, 44]. Homozygous, nonsynonymous polymorphisms in these genes were associated with a 5%–7% difference in recombination rate between lines ([Figure 4B](#)). There was, however, strong LD ($r^2 > 0.8$) between these alleles (e.g., lines with the lowest averaged crossover rates shared genotypic states for all three genes), and thus disentangling their independent effects on recombination rate was not possible. We also note that the small number of lines examined here precluded more powerful association methods (e.g., full genome-wide association study [GWAS]), and further work will be required to experimentally validate the contribution of these genes to variation in recombination rate.

Structural Variation Does Not Explain Differences in Recombination Rate

Both short and long-read sequencing revealed extensive structural variation between inbred lines of *D. pseudoobscura*. As expected, the three strategies we used to detect structural variation (GATK INDELS, PacBio SV and LUMPY/Smoove) varied in

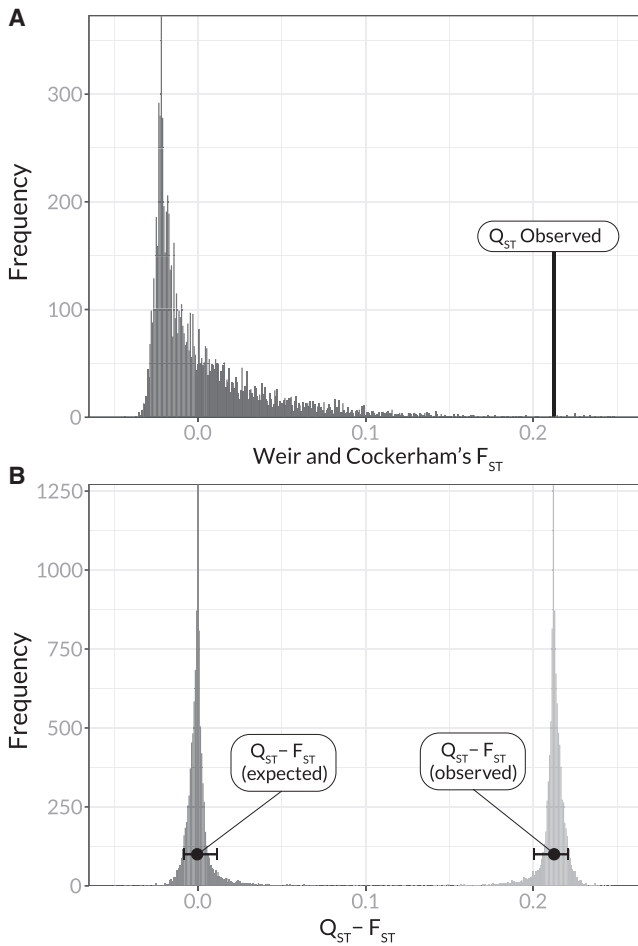


Figure 3. Recombination Rate $Q_{ST}-F_{ST}$ Exceeds Neutral Expectations

(A) Weir and Cockerham's F_{ST} from 6,591 RADseq-derived SNPs (mean F_{ST} = 0.0039). The observed value of Q_{ST} for recombination rate (0.212) is indicated with an arrow.

(B) Comparisons of the sampling distribution of $Q_{ST}-F_{ST}$ expected under neutrality and the observed value. Both distributions were simulated via a parametric bootstrap (see text). Black points with error bars indicate the mean and 95% confidence interval of the sampling distributions.

the number and relative proportions of the various classes of structural variant they identified (Figure S6). That said, all three methods suggested that the most common form of structural variation are small to mid-sized (10–100 bp) INDELs, with larger deletions, insertions, and duplications being much rarer (Figure S6). Consistent with the observation that AFC and MC are highly similar in their chromosomal arrangements, our structural variant analysis found no evidence of large-scale chromosomal inversions differentiating any of the lines.

Structural variation between lines did not co-vary with recombination rate (Figure 5). First, there was no relationship between recombination rate and the estimated percent sequence homology between the tester and inbred lines (Figure 5B, likelihood ratio test comparison of GLMMs, $df = 3$, $p = 0.3989$). Second, there was no relationship between recombination rate and the count of differences in structural alleles between each inbred

line and the tester line (Figure 5A, likelihood ratio test comparison of GLMMs, $df = 3$, $p = 0.7617$). This result was consistent across all methods used to identify structural variation (likelihood ratio tests, comparison of GLMMs with and without method by count/homology interaction effects, all $p > 0.3$). As such, at the 300 kb scale, there is no evidence that the local differences in recombination rate among inbred lines are a result of differences in homology or local genome structure.

DISCUSSION

Recombination rate is a key modulator of many evolutionary processes, yet we have a poor understanding of how recombination rate itself evolves. Here, we studied how recombination rate varies using strains from two natural populations of *D. pseudoobscura* from Madera Canyon, AZ, and American Fork Canyon, UT. We directly measured recombination rate in a total of 17 inbred lines from these populations and found substantial variation for recombination rate both within and between populations. Interestingly, the population from Madera Canyon, AZ, exhibited an ~8% lower recombination rate on average than the population from American Fork Canyon, UT. Within- and between-population variation in recombination rate manifested largely as differences in genome-wide recombination rate, rather than changes in the local recombination landscape. This finding is supported by a general pattern of covariation in recombination rate among chromosomes within lines. That said, our choice to assay greater numbers of individuals in fewer genomic intervals prevents us from ruling out the possibility of finer-scale differences in the recombination landscape between populations and lines. While overall differences in recombination rates between populations were modest in absolute terms (~8% depending on the interval), a $Q_{ST}-F_{ST}$ analysis revealed that this difference vastly exceeds the amount of phenotypic divergence expected under neutral drift. This result is consistent with the hypothesis that local adaptation has driven differences in recombination rate between these populations.

We explored two possible mechanisms underlying recombination rate differences between lines. First, we found evidence that some differences in recombination rate between lines may involve nonsynonymous coding changes in meiosis-related genes. Second, we found that local variation in recombination rate between lines does not correlate with local structural variation at the 300 kb scale. These findings suggest that the differences in recombination we observed were driven by alleles resulting in genome-wide changes in recombination rate rather than local remodeling of the recombination landscape. Below, we discuss the relevance of our findings for the study of the evolution of recombination rate and relationships to previous work.

Recombination Rate Variation in Natural Populations

Previous work has shown that recombination can vary between individuals, or between populations/species [25, 26, 45–47]. These studies have ranged from early work on chiasma frequency in snails [48] to more recent work leveraging modern human population genomic data [49, 50]. The bulk of this work has focused on describing variation in recombination and its potential molecular correlates. Further, most studies of natural populations have measured recombination in uncontrolled

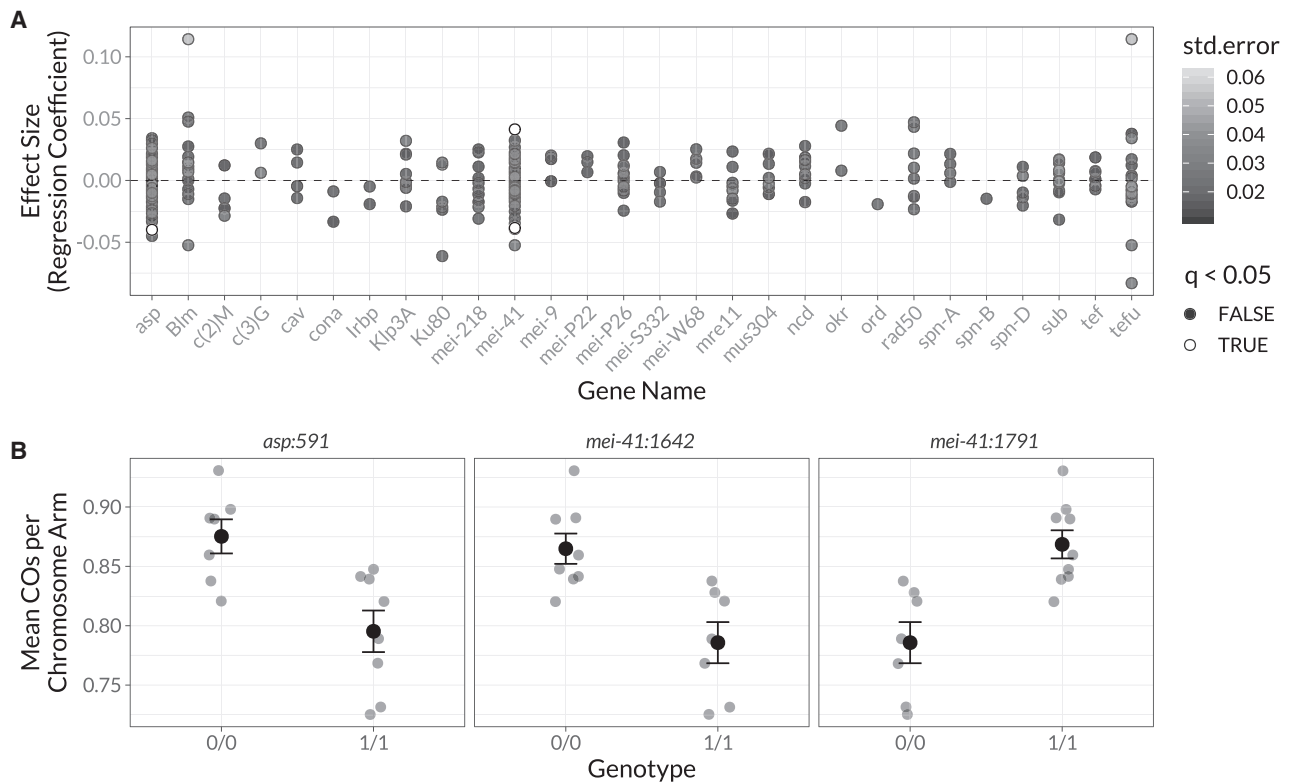


Figure 4. Nonsynonymous Substitutions Associated with Variation in Recombination Rate

(A) Regression coefficients from linear models (y axis) comparing genotype and crossover rate for sites (points) bearing nonsynonymous, non-reference polymorphisms in a collection of meiosis-related candidate genes (x axis). White points indicate associations that were significant after adjustment via FDR correction (adjusted $p < 0.05$).

(B) Mean recombination rates (crossovers per chromosome arm) for sites with significant associations (red points in A). Each panel depicts the mean and 95% confidence interval for crossover rates for each genotypic class (either 0/0, homozygous reference or 1/1, homozygous nonsynonymous non-reference).

See Table S3 for list of candidate genes. See Figure S3 for an example of GLMM model fit diagnostics.

environments (e.g., in the wild [25]). Our study contributes to this literature directly examining genetic variation for recombination rate both within and between natural populations of a single species and performing one of the first tests that this variation is shaped by natural selection. Together with previous work, our study contributes to a growing body of evidence that there is ample genetic variation for recombination rate in natural populations and that recombination rate is actively evolving on observable timescales.

Second, we found that recombination rate varies primarily at the genome-wide scale rather than via variation in specific genomic regions. Our candidate gene analysis suggests that this variation in genome-wide recombination rate may be the result of allelic variation in meiosis-related genes (i.e., *asp* and *mei-41*). This is in line with previous work connecting genetic variation in genes regulating meiosis and/or crossover formation to variation in variation in genome-wide recombination rate [29, 47, 49, 51, 52]. The emerging evidence for natural variation in gene-wide modifiers of recombination is particularly intriguing given that many theoretical models of recombination evolution make use of abstract “modifier” alleles that alter genome-wide rates of recombination [5, 6]. Further characterization of such modifiers in natural populations may eventually

allow direct tests of theoretical models of recombination evolution [2].

Local Adaptation of Recombination Rate

Our Q_{ST} - F_{ST} analysis suggests that differences in recombination rate between *Drosophila pseudoobscura* populations from AZ and UT may have been driven by natural selection. To our knowledge, this is the first application of the Q_{ST} - F_{ST} method to the study of recombination and among the first evidence for the role of selection acting on genome-wide recombination rate in natural populations [40]. However, while our results suggest a role for natural selection, the agent of selection underlying this change remains unknown. There are a wide variety of possible explanations for this difference [2]. For example, differences in recombination between the populations may be directly favored, or other phenotypic differences may be divergently selected between the populations that incidentally affect recombination rate (via linkage or pleiotropy). One intriguing possibility is local differences in climate: recombination rate in *Drosophila* is known to be plastic with respect to ambient temperature [53]. Madera Canyon, AZ, has a mean annual temperature of approximately eleven degrees Celsius higher than American Fork Canyon, UT (10.5°C versus 21.6°C [54]). Assuming that the temperature

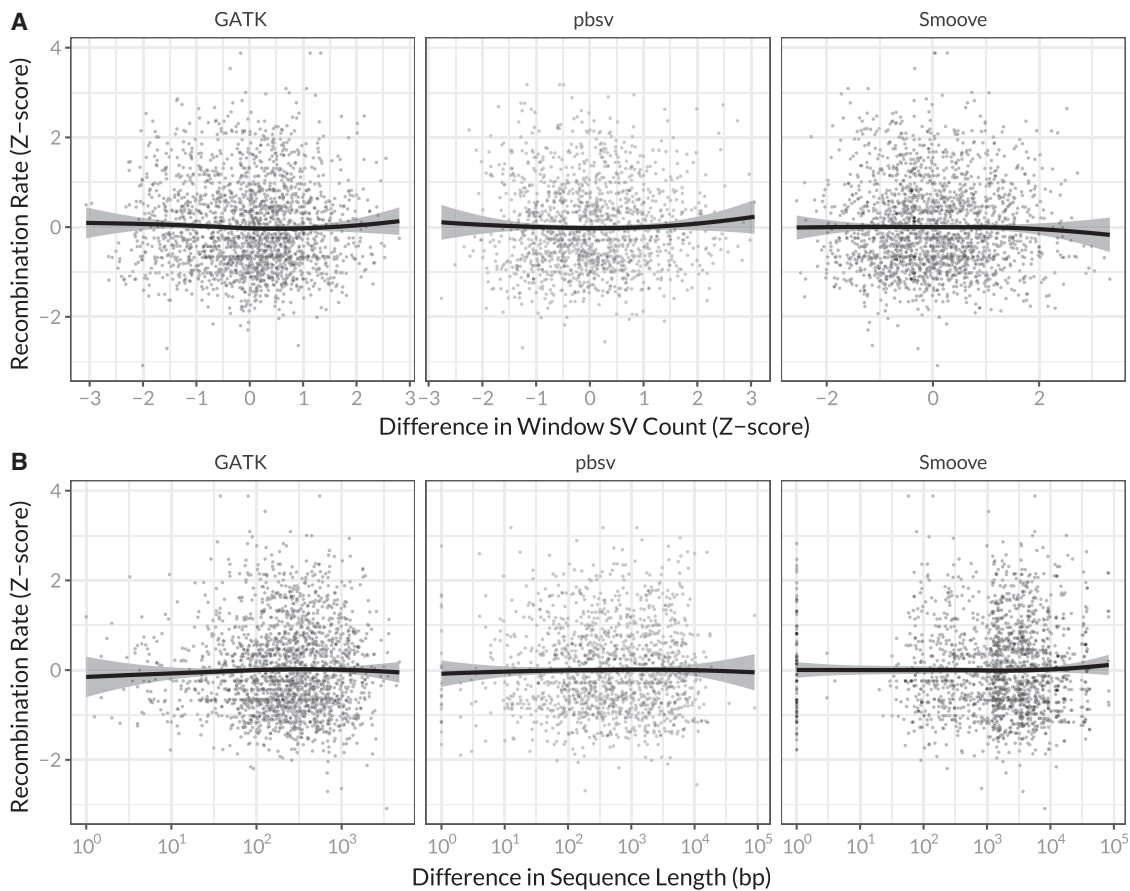


Figure 5. Structural Variation Is Not Correlated with Recombination Rate at the 300 kb Scale

(A) The relationship between normalized recombination rate and the normalized count of structural differences between each inbred line and the tester line. Each point represents a single recombination interval (all approximately 300 kb in length) from one inbred line. Lines on each plot represent smoothed conditional means and are accompanied by 95% confidence intervals. Each column depicts the relationship using each of the three methods used to assay structural variation.

(B) As in (A), but depicting the relationship between normalized recombination rate and the difference in total sequence length between each inbred line and the tester line.

See [Figure S3](#) for an example of GLMM model fit diagnostics. See [Figure S6](#) for a detailed summary of the frequency and size of different classes of structural variation.

reaction norm is similar in both populations, this higher temperature could, for example, cause an increase in realized recombination rate in the Madera Canyon population in the wild. We speculate that the difference in recombination rate we observed under constant conditions may be a compensatory response to an environmentally induced increase in recombination rate in order to return genome-wide recombination rate to some optimum value (i.e., a response to maladaptive plasticity [55]). Further work will naturally be needed to connect variation in recombination rates to specific agents of selection. One obvious extension of our approach would be a greater number of populations, perhaps existing over a climatic gradient (or paired populations in differing environments). We hope that our demonstration of the efficacy of the Q_{ST} - F_{ST} method inspires the undertaking of such eco-evolutionary studies of recombination rate.

One caveat regarding our application of the Q_{ST} - F_{ST} method is that our estimates of recombination come from F1s, and we were thus only able to observe genetic variation underlain by dominant

and co-dominant effects. This is not ideal, as it potentially alters the distribution of Q_{ST} relative to F_{ST} , which could bias the outcome of the Q_{ST} - F_{ST} test [35]. A dedicated simulation study aimed at understanding the direction and magnitude of this bias would be of great utility for future work on recombination using inbred lines.

Structural Variation as a Modulator of Recombination Rate

We found no association between among-line variation in recombination rate and among-line variation in the abundance or size of structural variants. An important consideration here is that this analysis was not intended to test whether average recombination rate (across all lines) is associated with structural variation—this association is extremely well documented and is unquestionably present in our data [56–58]. Instead, our goal was to test whether among-line variation in recombination rate in each genomic interval was explained by among-line structural

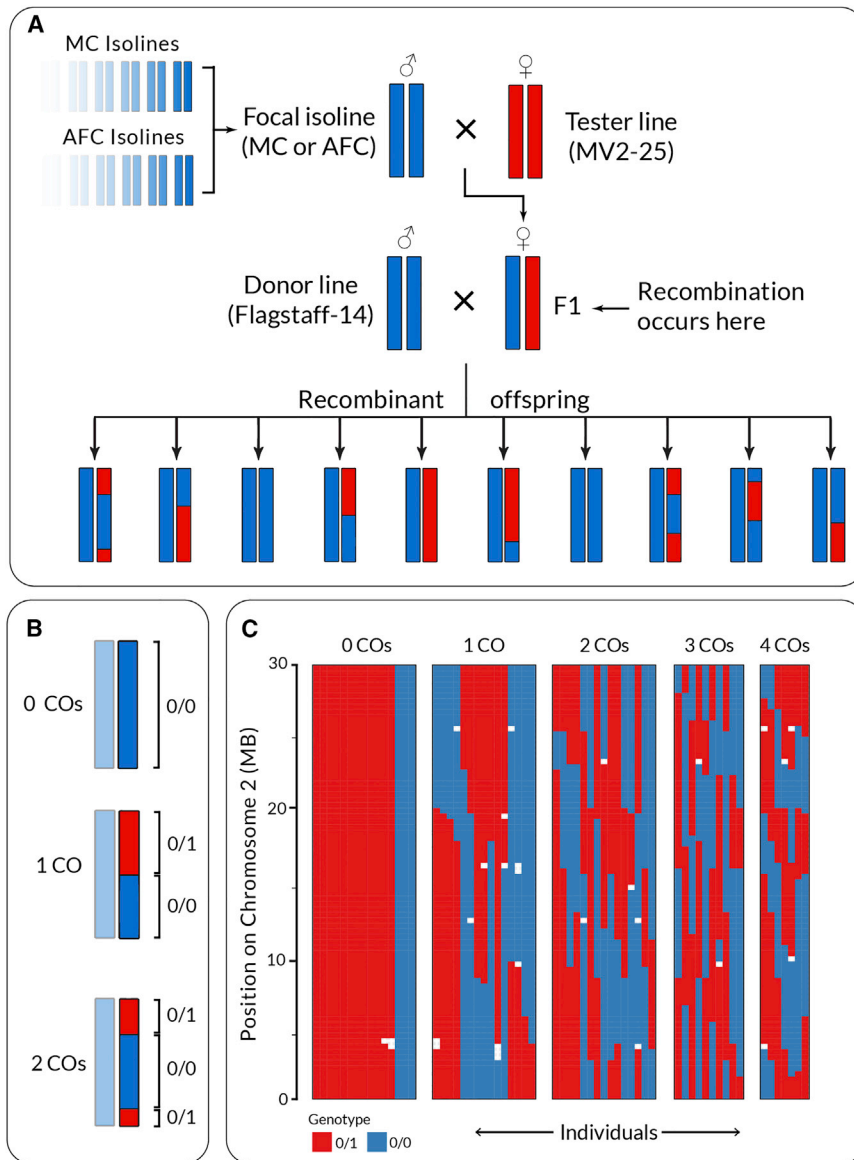


Figure 6. Schematic of the Crossing Design and One Method of Interfering Crossovers

(A) Isolines from MC and AFC were individually crossed to tester lines to generate F1s, which were subsequently crossed to a “donor line” sharing the same genotype as all isolines, but a different genotype than the tester line at all marker loci. (B) Further, all markers were selected such that only two alleles were found in all lines, with the tester line having one allele (“1”) and all other lines including the donor line having the other (“0”). As shown, this allows for the scoring of crossovers as changes in heterozygosity.

(C) Example genotypic data from one chromosome showing the number of inferred crossovers. White genotype states indicate missing data. See also Figure S1 for details on the performance of GT-seq and Table S4 for GT-seq primer sequences.

to this is large-scale chromosomal inversions (notably absent in our lines), which are well known to affect recombination at scales much larger than 300 kb—upward of 10 Mb in many cases [60, 61]. However, inversions likely have outsized recombination suppressing effects compared to other forms of non-homology because of the loop structures they form during chromosome pairing [60, 62]. Further work will be required to disentangle the relative contribution of structural and global/trans modifiers of recombination rate at different genomic scales.

Amplicon Sequencing as a Tool for Genetic Maps

Our ability to economically sequence hundreds of markers in thousands of individuals was made possible by the genotyping-in-thousands by sequencing

differences, using normalized metrics of both recombination rate and structural variation within each genomic interval (as Z scores, i.e., statistical controlling for average recombination rate).

Why was there no detectable association between structural variation and local rates of recombination? For one, our F1 cross design is not able to detect recessive-acting effects of structural variation (e.g., those that only affect recombination in homozygous form). Second, a key consideration in interpreting these results is the *scale* of our recombination estimates: much of the previous work describing the effects of heterozygous structural variation on crossing-over was performed at much finer scale, e.g., <1 kb in *Arabidopsis* [59]. It may be that changes in recombination resulting from structural variation are restricted to finer genomic scales (i.e., <300 kb) and that other types of regulators (e.g., variation in meiosis genes or the chromatin landscape) modulate recombination at larger scale [40]. A notable exception

(GT-seq) amplicon sequencing approach [63]. This technique is highly scalable, and, in our case, we likely could have sequenced many more markers (and/or individuals) while maintaining a very high depth per amplicon. This method is an alternative to the increasingly popular bulk-sequencing approaches, in which sample DNA is pooled prior to sequencing [64]. GT-seq avoids some of the complexity of these approaches. For one, because it is a PCR-based method, GT-seq does not require performing extraction, quantification, and manual normalization of sample DNA. This is a non-trivial consideration when individual sample sizes are in the thousands. Further, unlike bulk sequencing, amplicon sequencing provides individual-level genotypes. As such, the occurrence of double, triple, etc. crossovers can be directly resolved, and problematic individuals can be identified and removed during analyses. To our knowledge, these are both not currently possible with bulk sequencing (unless barcodes are employed,

limiting the total number of individuals in the pool). The main drawbacks of amplicon sequencing are a decrease in resolution (number of markers) and the need to pre-identify mapping informative markers. That said, we believe GT-seq and amplicon sequencing more generally will be a useful tool for future studies of variation in recombination rate and can be readily paired with other approaches depending on the goals of the study.

Conclusions

Recombination rate plays an important modulatory role in many evolutionary processes, but little is known about how recombination rate itself evolves. Here, we studied natural variation in recombination rate within and between two populations of *Drosophila pseudoobscura*. We found extensive genetic variation for recombination rate within and between populations, with the majority of variation detected manifesting as differences in overall genome-wide recombination rate. This suggests that the differences in recombination we detected between lines may be the result of genetic variation in *trans*-acting global regulators of recombination, an idea supported by a significant association between nonsynonymous variation in meiosis-associated genes and recombination rate. We also found no evidence that among-line differences in local recombination rate at the 300 kb scale were correlated with structural variation within the lines. Finally, we discovered that the magnitude of phenotypic difference in recombination rate between the two populations was far greater than expected under a model of neutral trait evolution, suggesting that the differences may have been driven by natural selection. Our study provides key insights in the quantitative genetics of recombination rate and lays the groundwork for future research focused on studying the recombination rate in natural populations.

STAR★METHODS

Detailed methods are provided in the online version of this paper and include the following:

- **KEY RESOURCES TABLE**
- **LEAD CONTACT AND MATERIALS AVAILABILITY**
- **EXPERIMENTAL MODEL AND SUBJECT DETAILS**
- **METHOD DETAILS**
 - RAD-seq libraries from wild samples
 - Whole genome sequencing of inbred lines
 - Whole genome variant calling: short read WGS and RAD-seq data
 - Creation of mapping populations
 - Genotyping of mapping populations
 - Detection of recombination events
 - Candidate genes associated with recombination differences
 - Association between local structural variation and recombination rate
- **QUANTIFICATION AND STATISTICAL ANALYSIS**
 - Population differences in recombination rate
 - QST-FST Analysis
 - Candidate genes associated with recombination differences

- Association between local structural variation and recombination rate
- **DATA AND CODE AVAILABILITY**

SUPPLEMENTAL INFORMATION

Supplemental Information can be found online at <https://doi.org/10.1016/j.cub.2020.03.053>.

ACKNOWLEDGMENTS

Funding for this project was provided by National Science Foundation grants DEB-1545627, 1754022, and 1754439 to M.A.F.N. K.S. was additionally supported by a Natural Sciences and Engineering Research Council of Canada Postdoctoral Fellowship. The tester line (MV2-25) was generously provided by Dr. Steven Schaeffer. We thank Dr. Noah Whiteman and Dr. John Chaston for assistance during fieldwork. Dr. Katharine Korunes, Dr. Jenn Coughlan, members of the Noor Lab, and three anonymous reviewers provided valuable feedback on the manuscript. Dr. Andrew MacDonald provided guidance on statistical analyses. Dr. Armin Töpfer provided advice on the use of the pbsv software.

AUTHOR CONTRIBUTIONS

Conceptualization, M.A.F.N. and K.S.; Methodology, K.S., B.M.-W., K.R.R., and M.A.F.N.; Software, K.S.; Formal Analysis, K.S.; Investigation, K.S., B.M.-W., and K.R.R.; Resources, M.A.F.N. and B.M.-W.; Data Curation, K.S.; Writing – Original Draft, K.S.; Writing – Review & Editing, K.S., M.A.F.N., B.M.-W., and K.R.R.; Visualization, K.S.; Supervision, M.A.F.N.; Project Administration, K.S. and B.M.-W.; Funding Acquisition, M.A.F.N. and K.S.

DECLARATION OF INTERESTS

The authors declare no competing interests.

Received: October 7, 2019

Revised: December 16, 2019

Accepted: March 20, 2020

Published: April 9, 2020

REFERENCES

1. Hughes, S.E., Miller, D.E., Miller, A.L., and Hawley, R.S. (2018). Female meiosis: synopsis, recombination, and segregation in *Drosophila melanogaster*. *Genetics* *208*, 875–908.
2. Dapper, A.L., and Payseur, B.A. (2017). Connecting theory and data to understand recombination rate evolution. *Philos. Trans. R. Soc. Lond. B Biol. Sci.* *372*, 20160469.
3. Charlesworth, B., Betancourt, A.J., Kaiser, V.B., and Gordo, I. (2009). Genetic recombination and molecular evolution. *Cold Spring Harb. Symp. Quant. Biol.* *74*, 177–186.
4. Ritz, K.R., Noor, M.A.F., and Singh, N.D. (2017). Variation in recombination rate: adaptive or not? *Trends Genet.* *33*, 364–374.
5. Otto, S.P., and Barton, N.H. (1997). The evolution of recombination: removing the limits to natural selection. *Genetics* *147*, 879–906.
6. Lenormand, T., and Otto, S.P. (2000). The evolution of recombination in a heterogeneous environment. *Genetics* *156*, 423–438.
7. Marais, G., and Charlesworth, B. (2003). Genome evolution: recombination speeds up adaptive evolution. *Curr. Biol.* *13*, R68–R70.
8. Martin, S.H., Davey, J.W., Salazar, C., and Jiggins, C.D. (2019). Recombination rate variation shapes barriers to introgression across butterfly genomes. *PLoS Biol.* *17*, e2006288.
9. Barton, N.H. (2010). Mutation and the evolution of recombination. *Philos. Trans. R. Soc. Lond. B Biol. Sci.* *365*, 1281–1294.

10. Charlesworth, B. (1976). Recombination modification in a fluctuating environment. *Genetics* 83, 181–195.
11. Kirkpatrick, M., and Barton, N. (2006). Chromosome inversions, local adaptation and speciation. *Genetics* 173, 419–434.
12. Noor, M.A.F., Grams, K.L., Bertucci, L.A., and Reiland, J. (2001). Chromosomal inversions and the reproductive isolation of species. *Proc. Natl. Acad. Sci. USA* 98, 12084–12088.
13. Samuk, K., Owens, G.L., Delmore, K.E., Miller, S.E., Rennison, D.J., and Schluter, D. (2017). Gene flow and selection interact to promote adaptive divergence in regions of low recombination. *Mol. Ecol.* 26, 4378–4390.
14. Schumer, M., Xu, C., Powell, D.L., Durvasula, A., Skov, L., Holland, C., Blazier, J.C., Sankararaman, S., Andolfatto, P., Rosenthal, G.G., and Przeworski, M. (2018). Natural selection interacts with recombination to shape the evolution of hybrid genomes. *Science* 360, 656–660.
15. Wang, R.J., and Payseur, B.A. (2017). Genetics of genome-wide recombination rate evolution in mice from an isolated island. *Genetics* 206, 1841–1852.
16. Kulathinal, R.J., Bennett, S.M., Fitzpatrick, C.L., and Noor, M.A. (2008). Fine-scale mapping of recombination rate in *Drosophila* refines its correlation to diversity and divergence. *Proc. Natl. Acad. Sci. USA* 105, 10051–10056.
17. Stumpf, M.P.H., and McVean, G.A.T. (2003). Estimating recombination rates from population-genetic data. *Nat. Rev. Genet.* 4, 959–968.
18. Wall, J.D. (2000). A comparison of estimators of the population recombination rate. *Mol. Biol. Evol.* 17, 156–163.
19. Auton, A., and McVean, G. (2007). Recombination rate estimation in the presence of hotspots. *Genome Res.* 17, 1219–1227.
20. Gärtner, K., and Futschik, A. (2016). Improved versions of common estimators of the recombination rate. *J. Comput. Biol.* 23, 756–768.
21. Adrion, J.R., Galloway, J.G., and Kern, A.D. (2019). Inferring the landscape of recombination using recurrent neural networks. *bioRxiv*. <https://doi.org/10.1101/662247>.
22. Nei, M., and Li, W.H. (1973). Linkage disequilibrium in subdivided populations. *Genetics* 75, 213–219.
23. Cutter, A.D. (2019). Recombination and linkage disequilibrium in evolutionary signatures. *A Primer of Molecular Population Genetics* (Oxford University Press), pp. 113–128.
24. McVean, G. (2007). Linkage disequilibrium, recombination and selection. In *Handbook of Statistical Genetics*, D.J. Balding, M. Bishop, and C. Cannings, eds. (Wiley), pp. 909–944.
25. Stapley, J., Feulner, P.G.D., Johnston, S.E., Santure, A.W., and Smadja, C.M. (2017). Variation in recombination frequency and distribution across eukaryotes: patterns and processes. *Philos. Trans. R. Soc. Lond. B Biol. Sci.* 372, 20160455.
26. Johnston, S.E., Bérénos, C., Slate, J., and Pemberton, J.M. (2016). Conserved genetic architecture underlying individual recombination rate variation in a wild population of soay sheep (*Ovis aries*). *Genetics* 203, 583–598.
27. Hellsten, U., Wright, K.M., Jenkins, J., Shu, S., Yuan, Y., Wessler, S.R., Schmutz, J., Willis, J.H., and Rokhsar, D.S. (2013). Fine-scale variation in meiotic recombination in *Mimulus* inferred from population shotgun sequencing. *Proc. Natl. Acad. Sci. USA* 110, 19478–19482.
28. Smukowski, C.S., and Noor, M.A.F. (2011). Recombination rate variation in closely related species. *Heredity* 107, 496–508.
29. Hunter, C.M., Huang, W., Mackay, T.F.C., and Singh, N.D. (2016). The genetic architecture of natural variation in recombination rate in *Drosophila melanogaster*. *PLoS Genet.* 12, e1005951.
30. Dumont, B.L., and Payseur, B.A. (2008). Evolution of the genomic rate of recombination in mammals. *Evolution* 62, 276–294.
31. Otto, S.P., and Michalakis, Y. (1998). The evolution of recombination in changing environments. *Trends Ecol. Evol.* 13, 145–151.
32. Aggarwal, D.D., Rashkovetsky, E., Michalak, P., Cohen, I., Ronin, Y., Zhou, D., Haddad, G.G., and Korol, A.B. (2015). Experimental evolution of recombination and crossover interference in *Drosophila* caused by directional selection for stress-related traits. *BMC Biol.* 13, 101.
33. Leinonen, T., McCairns, R.J., O’Hara, R.B., and Merilä, J. (2013). Q(ST)-F(ST) comparisons: evolutionary and ecological insights from genomic heterogeneity. *Nat. Rev. Genet.* 14, 179–190.
34. Whitlock, M.C. (2008). Evolutionary inference from QST. *Mol. Ecol.* 17, 1885–1896.
35. Whitlock, M.C., and Guillaume, F. (2009). Testing for spatially divergent selection: comparing QST to FST. *Genetics* 183, 1055–1063.
36. Barrett, R.D.H., and Hoekstra, H.E. (2011). Molecular spandrels: tests of adaptation at the genetic level. *Nat. Rev. Genet.* 12, 767–780.
37. Morgan, A.P., Gatti, D.M., Najarian, M.L., Keane, T.M., Galante, R.J., Pack, A.I., Mott, R., Churchill, G.A., and de Villena, F.P.-M. (2017). Structural variation shapes the landscape of recombination in mouse. *Genetics* 206, 603–619.
38. Völker, M., Backström, N., Skinner, B.M., Langley, E.J., Bunzey, S.K., Ellegren, H., and Griffin, D.K. (2010). Copy number variation, chromosome rearrangement, and their association with recombination during avian evolution. *Genome Res.* 20, 503–511.
39. Gaut, B.S., Wright, S.I., Rizzon, C., Dvorak, J., and Anderson, L.K. (2007). Recombination: an underappreciated factor in the evolution of plant genomes. *Nat. Rev. Genet.* 8, 77–84.
40. Brand, C.L., Cattani, M.V., Kingan, S.B., Landeen, E.L., and Presgraves, D.C. (2018). Molecular evolution at a meiosis gene mediates species differences in the rate and patterning of recombination. *Curr. Biol.* 28, 1289–1295.
41. Baker, Z., Schumer, M., Haba, Y., Bashkirova, L., Holland, C., Rosenthal, G.G., and Przeworski, M. (2017). Repeated losses of PRDM9-directed recombination despite the conservation of PRDM9 across vertebrates. *eLife* 6, e24133.
42. Petit, M., Astruc, J.-M., Sarry, J., Drouilhet, L., Fabre, S., Moreno, C.R., and Servin, B. (2017). Variation in recombination rate and its genetic determinism in sheep populations. *Genetics* 207, 767–784.
43. Wakefield, J.G., Bonaccorsi, S., and Gatti, M. (2001). The *Drosophila* protein asp is involved in microtubule organization during spindle formation and cytokinesis. *J. Cell Biol.* 153, 637–648.
44. Joyce, E.F., Pedersen, M., Tiong, S., White-Brown, S.K., Paul, A., Campbell, S.D., and McKim, K.S. (2011). *Drosophila* ATM and ATR have distinct activities in the regulation of meiotic DNA damage and repair. *J. Cell Biol.* 195, 359–367.
45. Bauer, E., Falque, M., Walter, H., Bauland, C., Camisan, C., Campo, L., Meyer, N., Ranc, N., Rincet, R., Schipprack, W., et al. (2013). Intraspecific variation of recombination rate in maize. *Genome Biol.* 14, R103.
46. Chowdhury, R., Bois, P.R.J., Feingold, E., Sherman, S.L., and Cheung, V.G. (2009). Genetic analysis of variation in human meiotic recombination. *PLoS Genet.* 5, e1000648.
47. Ziolkowski, P.A., Underwood, C.J., Lambing, C., Martinez-Garcia, M., Lawrence, E.J., Ziolkowska, L., Griffin, C., Choi, K., Franklin, F.C.H., Martienssen, R.A., and Henderson, I.R. (2017). Natural variation and dosage of the HEI10 meiotic E3 ligase control *Arabidopsis* crossover recombination. *Genes Dev.* 31, 306–317.
48. Price, D.J., and Bantock, C.R. (1975). Marginal populations of *Cepaea nemoralis* (L.) on the Brendon Hills, England. II. Variation in chiasma frequency. *Evolution* 29, 278–286.
49. Kong, A., Thorleifsson, G., Stefansson, H., Masson, G., Helgason, A., Gudbjartsson, D.F., Jonsdottir, G.M., Gudjonsson, S.A., Sverrisson, S., Thorlacius, T., et al. (2008). Sequence variants in the RNF212 gene associate with genome-wide recombination rate. *Science* 319, 1398–1401.
50. Kong, A., Thorleifsson, G., Gudbjartsson, D.F., Masson, G., Sigurdsson, A., Jonasdottir, A., Walters, G.B., Jonasdottir, A., Gylfason, A., Kristinsson, K.T., et al. (2010). Fine-scale recombination rate differences between sexes, populations and individuals. *Nature* 467, 1099–1103.

51. Sandor, C., Li, W., Coppieters, W., Druet, T., Charlier, C., and Georges, M. (2012). Genetic variants in REC8, RNF212, and PRDM9 influence male recombination in cattle. *PLoS Genet.* *8*, e1002854.
52. Wang, R.J., Dumont, B.L., Jing, P., and Payseur, B.A. (2019). A first genetic portrait of synaptonemal complex variation. *PLoS Genet.* *15*, e1008337.
53. Jackson, S., Nielsen, D.M., and Singh, N.D. (2015). Increased exposure to acute thermal stress is associated with a non-linear increase in recombination frequency and an independent linear decrease in fitness in *Drosophila*. *BMC Evol. Biol.* *15*, 175.
54. Menne, M.J., Williams, C.N., Gleason, B.E., Rennie, J.J., and Lawrimore, J.H. (2018). The Global Historical Climatology Network Monthly Temperature dataset, version 4. *J. Clim.* *31*, 9835–9854.
55. King, J.G., and Hadfield, J.D. (2019). The evolution of phenotypic plasticity when environments fluctuate in time and space. *Evol. Lett.* *3*, 15–27.
56. Kawakami, T., Mugal, C.F., Suh, A., Nater, A., Burri, R., Smeds, L., and Ellegren, H. (2017). Whole-genome patterns of linkage disequilibrium across flycatcher populations clarify the causes and consequences of fine-scale recombination rate variation in birds. *Mol. Ecol.* *26*, 4158–4172.
57. Kent, T.V., Uzunović, J., and Wright, S.I. (2017). Coevolution between transposable elements and recombination. *Philos. Trans. R. Soc. Lond. B Biol. Sci.* *372*, 20160458.
58. Ross, C.R., DeFelice, D.S., Hunt, G.J., Ihle, K.E., Amdam, G.V., and Rueppell, O. (2015). Genomic correlates of recombination rate and its variability across eight recombination maps in the western honey bee (*Apis mellifera* L.). *BMC Genomics* *16*, 107.
59. Opperman, R., Emmanuel, E., and Levy, A.A. (2004). The effect of sequence divergence on recombination between direct repeats in *Arabidopsis*. *Genetics* *168*, 2207–2215.
60. Crown, K.N., Miller, D.E., Sekelsky, J., and Hawley, R.S. (2018). Local inversion heterozygosity alters recombination throughout the genome. *Curr. Biol.* *28*, 2984–2990.
61. Said, I., Byrne, A., Serrano, V., Cardeno, C., Vollmers, C., and Corbett-Detig, R. (2018). Linked genetic variation and not genome structure causes widespread differential expression associated with chromosomal inversions. *Proc. Natl. Acad. Sci. USA* *115*, 5492–5497.
62. Ortiz-Barrientos, D., Chang, A.S., and Noor, M.A.F. (2006). A recombinational portrait of the *Drosophila pseudoobscura* genome. *Genet. Res.* *87*, 23–31.
63. Campbell, N.R., Harmon, S.A., and Narum, S.R. (2015). Genotyping-in-thousands by sequencing (GT-seq): a cost effective SNP genotyping method based on custom amplicon sequencing. *Mol. Ecol. Resour.* *15*, 855–867.
64. Chakraborty, P., Pankajam, A.V., Dutta, A., and Nishant, K.T. (2018). Genome wide analysis of meiotic recombination in yeast: for a few SNPs more. *IUBMB Life* *70*, 743–752.
65. Li, H., Handsaker, B., Wysoker, A., Fennell, T., Ruan, J., Homer, N., Marth, G., Abecasis, G., and Durbin, R.; 1000 Genome Project Data Processing Subgroup (2009). The Sequence Alignment/Map format and SAMtools. *Bioinformatics* *25*, 2078–2079.
66. Li, H. (2013). Aligning sequence reads, clone sequences and assembly contigs with BWA-MEM. *arXiv*, 1303.3997. <http://arxiv.org/abs/1303.3997>.
67. Poplin, R., Chang, P.-C., Alexander, D., Schwartz, S., Colthurst, T., Ku, A., Newburger, D., Dijamco, J., Nguyen, N., Afshar, P.T., et al. (2018). A universal SNP and small-indel variant caller using deep neural networks. *Nat. Biotechnol.* *36*, 983–987.
68. Bunn, A., and Korpela, M. (2020). An introduction to dplR. <https://repo.bppt.go.id/cran/web/packages/dplR/vignettes/intro-dplR.pdf>.
69. RStudio (2015). RStudio: integrated development for R. <http://www.rstudio.com>.
70. Wickham, H. (2017). tidyverse: easily install and load the “Tidyverse”. <https://CRAN.R-project.org/package=tidyverse>.
71. Bates, D., Mächler, M., Bolker, B., and Walker, S. (2015). Fitting linear mixed-effects models using lme4. *J. Stat. Softw.* *67*, 1–48.
72. Broman, K.W., Wu, H., Sen, S., and Churchill, G.A. (2003). R/qtl: QTL mapping in experimental crosses. *Bioinformatics* *19*, 889–890.
73. Taylor, J., and Butler, D. (2017). R package ASMap: efficient genetic linkage map construction and diagnosis. *J. Stat. Softw.* *79*, 1–29.
74. Knaus, B.J., and Grünwald, N.J. (2017). vcfR: a package to manipulate and visualize variant call format data in R. *Mol. Ecol. Resour.* *17*, 44–53.
75. Pedersen, T.L. (2017). patchwork: the composer of ggplots. R package version 0.0.1. <https://cran.r-project.org/web/packages/patchwork/index.html>.
76. Zheng, X. (2012). SNPRelate: parallel computing toolset for genome-wide association studies. R package version 95. <https://github.com/zhengxwen/SNPRelate>.
77. Kuznetsova, A., Brockhoff, P.B., and Christensen, R.H.B. (2017). lmerTest package: tests in linear mixed effects models. *J. Stat. Softw.* *82*. Published online December 6, 2017. <https://doi.org/10.18637/jss.v082.i13>.
78. Fox, J., and Weisberg, S. (2018). *An R Companion to Applied Regression* (SAGE Publications).
79. Ritz, K.R., and Noor, M.A.F. (2015). North American Southwest collection of *obscura*-group *Drosophila* in summer 2015. *Drosoph. Inf. Serv.* *98* [http://www.ou.edu/journals/dis/DIS98/RitzNoor\(pg23\).pdf](http://www.ou.edu/journals/dis/DIS98/RitzNoor(pg23).pdf).
80. Peterson, B.K., Weber, J.N., Kay, E.H., Fisher, H.S., and Hoekstra, H.E. (2012). Double digest RADseq: an inexpensive method for de novo SNP discovery and genotyping in model and non-model species. *PLoS ONE* *7*, e37135.
81. DePristo, M.A., Banks, E., Poplin, R., Garimella, K.V., Maguire, J.R., Hartl, C., Philippakis, A.A., del Angel, G., Rivas, M.A., Hanna, M., et al. (2011). A framework for variation discovery and genotyping using next-generation DNA sequencing data. *Nat. Genet.* *43*, 491–498.
82. Van der Auwera, G.A., Carneiro, M.O., Hartl, C., Poplin, R., Del Angel, G., Levy-Moonshine, A., Jordan, T., Shakir, K., Roazen, D., Thibault, J., et al. (2013). From FastQ data to high confidence variant calls: the Genome Analysis Toolkit best practices pipeline. *Curr. Protoc. Bioinformatics* *43*, 11.10.1–33.
83. Li, H., and Durbin, R. (2009). Fast and accurate short read alignment with Burrows-Wheeler transform. *Bioinformatics* *25*, 1754–1760.
84. Wysocki, A., Tibbetts, K., and Fennell, T. (2013). Picard tools version 1.90. <http://picard.sourceforge.net>.
85. R Core Team (2018). R: A language and environment for statistical computing. <https://www.R-project.org/>.
86. Schaeffer, S.W., Bhutkar, A., McAllister, B.F., Matsuda, M., Matzkin, L.M., O’Grady, P.M., Rohde, C., Valente, V.L.S., Aguadé, M., Anderson, W.W., et al. (2008). Polytene chromosomal maps of 11 *Drosophila* species: the order of genomic scaffolds inferred from genetic and physical maps. *Genetics* *179*, 1601–1655.
87. Broman, K.W., and Sen, S. (2009). *A Guide to QTL Mapping with R/qtl* (Springer).
88. Anderson, J.A., Gilliland, W.D., and Langley, C.H. (2009). Molecular population genetics and evolution of *Drosophila* meiosis genes. *Genetics* *181*, 177–185.
89. Katoh, K., and Standley, D.M. (2013). MAFFT multiple sequence alignment software version 7: improvements in performance and usability. *Mol. Biol. Evol.* *30*, 772–780.
90. Korunes, K.L., and Noor, M.A.F. (2019). Pervasive gene conversion in chromosomal inversion heterozygotes. *Mol. Ecol.* *28*, 1302–1315.
91. Larson, D.E., Abel, H.J., Chiang, C., Badve, A., Das, I., Eldred, J.M., Lauer, R.M., and Hall, I.M. (2019). svtools: population-scale analysis of structural variation. *Bioinformatics* *35*, 4782–4787.

92. Tarasov, A., Vilella, A.J., Cuppen, E., Nijman, I.J., and Prins, P. (2015). Sambamba: fast processing of NGS alignment formats. *Bioinformatics* *31*, 2032–2034.
93. Faust, G.G., and Hall, I.M. (2014). SAMBLASTER: fast duplicate marking and structural variant read extraction. *Bioinformatics* *30*, 2503–2505.
94. Wenger, A.M., Peluso, P., Rowell, W.J., Chang, P.-C., Hall, R.J., Concepcion, G.T., Ebler, J., Fungtammasan, A., Kolesnikov, A., Olson, N.D., et al. (2019). Accurate circular consensus long-read sequencing improves variant detection and assembly of a human genome. *Nat. Biotechnol.* *37*, 1155–1162.
95. Greig, D., Travisano, M., Louis, E.J., and Borts, R.H. (2003). A role for the mismatch repair system during incipient speciation in *Saccharomyces*. *J. Evol. Biol.* *16*, 429–437.
96. Rogers, D.W., McConnell, E., Ono, J., and Greig, D. (2018). Spore-autonomous fluorescent protein expression identifies meiotic chromosome mis-segregation as the principal cause of hybrid sterility in yeast. *PLoS Biol.* *16*, e2005066.
97. Salomé, P.A., Bomblies, K., Fitz, J., Laitinen, R.A.E., Warthmann, N., Yant, L., and Weigel, D. (2012). The recombination landscape in *Arabidopsis thaliana* F2 populations. *Heredity* *108*, 447–455.
98. Bates, D., Sarkar, D., Bates, M.D., and Matrix, L. (2007). The lme4 package. R package version 2, 74.
99. Walsh, B., and Lynch, M. (2018). *Evolution and Selection of Quantitative Traits* (Oxford University Press).
100. Zheng, X., Levine, D., Shen, J., Gogarten, S.M., Laurie, C., and Weir, B.S. (2012). A high-performance computing toolset for relatedness and principal component analysis of SNP data. *Bioinformatics* *28*, 3326–3328.
101. Lotterhos, K.E. (2019). The effect of neutral recombination variation on genome scans for selection. G3: Genes|Genomes|Genetics, g3.400088.2019.
102. Benjamini, Y., and Hochberg, Y. (1995). Controlling the false discovery rate: a practical and powerful approach to multiple testing. *J. R. Stat. Soc. Series B Stat. Methodol.* *57*, 289–300.

STAR★METHODS

KEY RESOURCES TABLE

REAGENT or RESOURCE	SOURCE	IDENTIFIER
Biological Samples		
Flagstaff14	This study	N/A
MV2-25	Dr. Steven Schaeffer	N/A
American Fork Canyon Inbred Lines	This study	N/A
Madera Canyon Inbred Lines	This study	N/A
Chemicals, Peptides, and Recombinant Proteins		
QIAGEN Plus Multiplex PCR Master Mix	QIAGEN	Cat # 206145
Charm Biotech Just-A-Plate 96 PCR Purification and Normalization Kit	Charm Biotech	Cat # JN-120-10
AmpureXP beads	Beckman Coulter	Cat # A63881
Deposited Data		
PacBio Sequel Whole Genome Sequencing	This paper	SRA PRJNA610090
Illumina HiSeq Whole Genome Sequencing	This paper	SRA PRJNA610029
Illumina HiSeq ddRAD-seq Sequencing	This paper	SRA PRJNA610904
Illumina NovaSeq Amplicon Libraries (High Output)	This paper	Dryad Accession https://doi.org/10.5061/dryad.jsxksn062
Illumina NovaSeq Amplicon Libraries (Mid Output)	This paper	Dryad Accession https://doi.org/10.5061/dryad.jsxksn062
Analysis scripts	This paper	https://github.com/ksamuk/samuk_et_al_curr_biol_2020
Oligonucleotides		
GT-Seq Primers - See Table S4	This paper	N/A
Illumina Small RNA sequencing primer (CGACAGGTTCCAGAGTTCTACAGTCCGACGATC)	Illumina	N/A
Software and Algorithms		
samtools	[65]	http://www.htslib.org/
Bwa2	[66]	https://github.com/lh3/bwa
GATK	[67]	https://gatk.broadinstitute.org/hc/en-us
R for Statistical Programming	[68]	https://www.r-project.org/
RStudio	[69]	https://rstudio.com/
tidyverse (R Package collection)	[70]	https://www.tidyverse.org/
lme4 (R Package)	[71]	https://cran.r-project.org/web/packages/lme4/index.html
r/qtl (R Package)	[72]	https://rqt1.org/
ASmap (R Package)	[73]	https://cran.r-project.org/web/packages/ASMap/index.html
vcfR	[74]	https://cran.r-project.org/web/packages/vcfR/index.html
patchwork	[75]	https://cran.r-project.org/web/packages/patchwork/index.html
SNPRelate	[76]	https://github.com/zhengxwen/SNPRelate
lmerTest	[77]	https://cran.r-project.org/web/packages/lmerTest/index.html
car (R Package)	[78]	https://cran.r-project.org/web/packages/car/index.html

LEAD CONTACT AND MATERIALS AVAILABILITY

Further information and requests for resources and protocols should be directed to and will be fulfilled by the Lead Contact, Dr. Kieran Samuk (ksamuk@gmail.com). This study did not generate new unique reagents.

EXPERIMENTAL MODEL AND SUBJECT DETAILS

We collected wild male and female *Drosophila pseudoobscura* from Madera Canyon, AZ, USA (31°42′48.9″N, 110°52′22.4″W) and American Fork Canyon, UT, USA (40°26′38.9″N, 111°42′08.5″W) in May and July of 2015 respectively using bucket traps [79]. These populations were chosen because they were known to share similar karyotypic configurations (e.g., inversions) but also differ in their ecological context (i.e., xeric versus sub-alpine). We returned live individuals to the laboratory, isolated females, and created inbred lines from their offspring (one line per surviving female). These lines were created by successive crosses between virgin siblings for a minimum of 14 generations. The inbred lines (and all subsequent lines) were reared in 20C incubators with 65% relative humidity and photoperiods of 14D:10N. The inbreeding process resulted in a total of 7 inbred lines from Arizona and 12 from Utah.

METHOD DETAILS

RAD-seq libraries from wild samples

To generate a set of SNPs for estimating F_{ST} between the Utah and Arizona populations, we performed double-digest RAD-seq reduced representation sequencing. To begin, we extracted DNA from single wild-caught individuals (excluding the females used to initiate the inbred lines) via phenol-chloroform DNA extraction. We then performed a RAD-seq library preparation protocol after [80]. The resulting libraries were sequenced in a single lane on an Illumina HiSeq 4000 at the Duke Center for Genomic and Computational Biology sequencing facility.

Whole genome sequencing of inbred lines

We performed both short read and long read whole genome sequencing on all 17 inbred lines, as well as our testers line (MV2-25 and Flagstaff-14). The short read libraries were prepared by first performing phenol-chloroform DNA extractions from pools of 20-30 individual female flies. We quantified DNA purity and concentration via Nanodrop (ThermoFisher) and Qubit (QIAGEN). The DNA samples were then submitted for library preparation and sequencing via Illumina NovaSeq (300-400bp insert, 150bp paired end reads) at the Duke Center for Genomic and Computational Biology sequencing facility.

The long-read libraries were prepared by first performing high-molecular weight DNA extractions from pools of 20-30 female flies using QIAGEN Midi/Mini Prep DNA extraction kits (QIAGEN). These were then assessed for fragment size via standard gel electrophoresis and submitted for sequencing on a PacBio Sequel (4 SMRT cells, 4-5 samples multiplexed per cell) at the Duke Center for Genomic and Computational Biology sequencing facility.

Whole genome variant calling: short read WGS and RAD-seq data

We identified variants in the short read data (both isolate whole genome sequencing and wild population RAD-seq) using an analysis pipeline based on the GATK best practices [81, 82]. The complete code for this pipeline is available as a Github repository at http://github.com/ksamuk/samuk_et_al_curr_biol_2020. All tools were run with default settings unless otherwise indicated. Briefly, we aligned the reads for each sample to the *D. pseudoobscura* reference genome (version 3.04 from FlyBase, ftp://ftp.flybase.net/genomes/Drosophila_pseudoobscura/) using bwa mem version 0.7.17 [83]. We marked adapters and duplicates using PicardTools [84], and performed individual-level genotyping for each set of marked reads using the HaplotypeCaller. We then performed joint genotyping on the resulting set of GVCFs via GenotypeGVCFs. We filtered SNPs in the resulting VCF using the GATK Best Practices hard filters (see scripts for details), working in R 3.4.1 [85] with the vcfR and tidyverse packages [70, 74].

Creation of mapping populations

To estimate variation in crossover rate in our inbred lines, we created backcross-like mapping populations (crossing scheme shown in Figure 6). We crossed groups of 3-5 males from each isolate to single virgin females from the *D. pseudoobscura* reference genome isolate (MV2-25, provided by Dr. Steve Schaeffer). We then allowed the F_1 offspring to develop and collected virgin females from the resulting offspring. Finally, we crossed these virgin F_1 females to males from a second fixed isolate, Flagstaff-14 (a highly inbred isolate from Flagstaff, AZ). This resulted in a backcross-like mapping population for each of the AZ and UT lines, in which all BC1 offspring had one maternal chromosome from their F_1 mother and one paternal Flagstaff-14 chromosome with a fixed, known genotype (Figure 6A). This design allows for straightforward mapping of recombination events that occurred in F_1 females. As such, our estimates are unable to detect any variation in recombination due to recessive-acting effects and may underestimate total recombination rates (e.g., from modifiers that act in an additive fashion) in the pure inbred lines. Critically, this potential underestimation is identical across all F_1 families, and thus cannot (in and of itself) generate systematic differences in recombination rate between lines or populations.

Genotyping of mapping populations

Because our goal was to quantify the number of crossovers per generation rather than their precise location, we performed low density, genome-wide SNP genotyping using an amplicon sequencing approach. To do this, we adapted the ‘GT-seq’ method outlined in [63]. A summary of the design and performance of this method is depicted in Figure S1. To begin, we identified SNPs genotyped in the whole genome dataset that were unique to the MV2-25 isoline (i.e., fixed for one allele in all 19 inbred lines and Flagstaff-14 and fixed for another allele in MV2-25). Genotyping these markers in BC1 individuals allows the recovery of genotypic phase simply by examining the genotype of the marker SNPs – regions with UT or AZ ancestry are represented as runs of heterozygous SNPs and regions with MV2-25 ancestry are represented as runs of homozygous SNPs (see diagram in Figure 6B). In total, we selected 500 of these SNPs evenly spaced at approximately 300kb intervals along each chromosome (Figures S1A and S1B). Note that this choice of marker density is optimized to detect small differences in *genome wide* recombination rate and cannot completely resolve fine scale (i.e., < 300kb) variation in the recombination landscape.

We designed primer pairs to generate ~200-300bp amplicons containing each of our target SNPs. These primer pairs were optimized to minimize primer-primer interactions during multiplex PCR (primer design service provided by GT-Seek, Idaho, USA). With these primers in hand, we performed two test library preps using the GT-seq protocol described in Campbell et al. (2015). We sequenced the first test library on a MiSeq (V3 flow cell, Illumina, California, USA), and identified poorly performing amplicons using the criteria outlined in Campbell et al. (2015), i.e., high dropout, low representation among individuals, evidence of amplicons mapping to duplicate regions, etc. (service provided by GT-Seek LTD, Idaho, USA). We then prepared a second test library with the primers for the poor-performing amplicons omitted and sequenced it as above. A final screen for poor-performing amplicons resulted in a final set of 390 amplicons ranging from 200-300bp, each containing at least one recombination-informative SNP.

After optimizing our panel of amplicons, we used GT-seq to genotype approximately 400 BC1 offspring from each mapping population (400 individuals from each of 19 lines, a total of approximately 7600 individuals). We created two pools of 40 plates (individuals and plates are individually barcoded as part of GT-seq library preparation) and submitted these for sequencing on an Illumina NextSeq 500 (1st pool: High Output Reagent 150 PE Reagent Kit, 2nd Pool: Mid Output 150 PE Kit, Illumina, California) at the Duke Center for Genomic and Computational Biology sequencing facility. We called SNPs in our sequenced GT-seq amplicons using an identical approach to our whole genome short read data. The final dataset contained 679 total variants across all amplicons, sequenced to an average depth of ~200X (Figure S1C). While there was some variability in sequencing depth between amplicons (mean coefficient of variation for depth of amplicon sequence was ~0.75), the overall high depth of sequencing resulted in the vast majority of amplicons having > 100X coverage (Figure S1C). We performed further quality control on the resulting SNPs in R using the *vcfR* and *tidyverse* packages [70, 74]. First, we dropped any markers that mapped to genomic locations outside our original targeted amplicons. Next, we dropped any individuals that had an average depth below 10X (19/7600 individuals). Finally, we removed any markers that displayed any evidence that they were in fact not unique to the tester line. This was done by removing markers displaying: (1) any evidence of segregation distortion, (2) any evidence that any of the isolines were in fact polymorphic for the marker or (3) high dropout (i.e., represented in fewer than 75% of samples). In some cases, the source of marker dropout was clearly an undetected INDEL polymorphism in the amplified regions, which, for consistency among lines, we erred on the side of removing rather than recoding as them as markers for mapping. The final set contained 344 mapping-informative SNPs. After filtering, we recoded all SNP genotypes as ‘0’ for the isoline/donor line state and ‘1’ for the tester line state. Because of the backcross design, the only possible genotypes were thus ‘0/0’ and ‘0/1’.

Detection of recombination events

We identified crossovers in two steps: (1) ancestry assignment of chromosome segments and (2) crossover counting. To begin, we updated the genomic ordering of our markers using the genomic scaffold ordering from [86]. Note that this reordering results in movement and replacement of contigs between chromosomes, and as such overall physical lengths of the reordered chromosomes are different from that of the most current *D. pseudoobscura* reference (version 3.04). After markers had been reordered, we assigned the ancestry (isoline or tester) of chromosomal segments by identifying runs of 0/0 s and 0/1 s. In regions with a single ancestry assignment, we imputed (via parsimony) across gaps of missing markers (e.g., due to filtration or dropout) shorter than 2 markers (~400kb). After local ancestry was assigned, we counted crossovers by counting the number of ancestry changes (from 0/0 to 0/1) along each chromosome in each individual using the function *countXO* in *R/qtl* [52]. Following the recommendations in [87], we ignored double crossovers spanning less than 2 markers (~400kb) and/or individuals displaying more than four crossovers on a single chromosome: crossover interference should make close range double crossovers exceedingly rare, and thus these cases likely represent genotyping or marker-order errors. It is also worth noting that our method of crossover detecting relies on quantifying crossover events in live-born offspring. As such, any extreme changes in crossover patterns incompatible with proper chromosome segregation during meiosis will not be observed (i.e., because they are lethal or lead to gamete degradation).

This crossover counting method assumes that the order of markers on each chromosome is identical in each line. Differences in marker order could, for example, generate spurious double crossovers (although ignoring short double crossovers reduces this problem). To directly address the possibility of different marker orders among lines, we created separate genetic maps for each isoline using the R packages *r/QTL* and *ASMap* [73, 87]. Following the general recommendations from the documentation, these two

packages agnostically infer linkage group assignment, marker order, and genetic distances between markers. Overall, there was high concordance in marker order between all the individually-inferred maps (Figure S2). Individual recombination rate estimates within each line were highly similar when using the reference genome marker order or individually-inferred marker orders (Figure S2, Spearman rank correlation = 0.93, $p < 2.2 \times 10^{-16}$). We thus elected to use the reference genome marker order (reordered based on [86]) for all subsequent analyses. Individual estimates of crossover events are provided in Tables S1 and S2.

Candidate genes associated with recombination differences

We explored the possibility that between-line variation in meiosis-related candidate genes may underlie between-line differences in recombination rate. We were specifically interested in the hypothesis that coding changes in meiosis genes underlie any differences in recombination rate between inbred lines (and act dominantly or additively in the F₁s). To do this, we first assembled a list of candidate genes from Anderson et al., 2009 and Hunter et al., 2016 [29, 88] (full list in Table S3). We then obtained the FASTA sequences for these genes in each line by intersecting the short read variant calls (including INDELS) with the *D. pseudoobscura* reference genome CDS for each candidate gene. To ensure proper alignment, we then performed multiple alignment of the line-level FASTA sequences and the reference CDS using MAFFT version 7.407 [89]. Once the sequences had been aligned, we identified non-synonymous, non-reference alleles in each line.

Association between local structural variation and recombination rate

Along with the candidate gene approach to examine associations with genome-wide recombination rate, we also investigated the possibility that small-scale differences in genomic structure between the inbred lines may explain differences in recombination rate. This may be of particular importance given that our design required measuring recombination rate in F₁ individuals (inbred line × tester line), and that structural heterozygosity has a well-known negative association with recombination rate [37, 60, 90].

To test if differences in genome structure underlie local differences in recombination rate in our inbred lines, we first identified structural variants (SVs) using two approaches. First, we used the SVtools pipeline [91] to identify SVs using paired-end short read data. This pipeline identifies structural variation using a variety of genomic signatures, particularly split reads (different parts of a single read mapping to multiple discrete locations) and discordant reads (paired end reads separated by a much greater genomic distance than expected on the basis of their insert size). SVtools can identify insertions, deletions, inversions, duplications, and other classes of rearrangements. The general procedure is to identify split/discordant reads using the tools SAMBAMBA and SAMBLASTER, which are then analyzed and annotated with the SVtools variant callers [92, 93]. The resulting structural variant VCF was filtered via empirical cutoffs using the guidelines in [91]. Along with SVtools, we separately identified structural variation in the PacBio long reads dataset using the PacBio structural variant pipeline and tools, pbsv (<https://github.com/PacificBiosciences/pbsv>, see also [94]). This involves aligning the long reads with *minimap2* (accessed via the *pbmm2* wrapper), identifying individual signatures of structural variation using pbsv, and jointly calling structural variation from the combined set of signatures. This again results in a VCF containing structural variants, which we filtered using empirical cutoffs as before.

After identifying structural variants, we next quantified the total difference in sequence homology between each line and the tester line (MV2-25) for each genomic interval where recombination was measured (~300kb windows). To do this, we summed the total number of non-shared, non-reference base pairs between each line and the tester line. We included SNPs, inversions, insertions, deletions, and translocations in this calculation. This method collapses multiple classes of genomic variation into a single, consistent metric and avoids the ambiguity associated with identifying shared locations of breakpoints for the structural variants (e.g., needed for per-variant associations). Further, this method focuses on the most likely biological cause of structurally-mediated recombination suppression, i.e., differences in homology per se, which has been widely demonstrated in many species [95–97]. We also tabulated the total count of structural variant alleles (of any type) that differed between each isolate and the tester line for each recombination interval. We normalized all homology estimates and structural variant counts in each window using both the total number of genotyped base pairs in each window as well as the mean depth per isolate.

QUANTIFICATION AND STATISTICAL ANALYSIS

Population differences in recombination rate

We quantified differences in recombination rate between populations using a generalized linear mixed model fitted with the R package *lme4* [98]. This model had the form $crossover\ count \sim population + (1|inbred\ line)$, with a Poisson error distribution and a log link function (in order to accommodate the non-normal nature of crossover counts). We checked for violations of model fit for this and all subsequent models using a QQ-plot and a fitted versus Pearson residuals plot (see Figure S3 for an example). To test the fixed effect of population, we performed a Type II Wald Test using the function “Anova” from the *car* package [78], as well as a Likelihood Ratio Test comparing models with and without the population term. Note that these two tests focus on a slightly different hypothesis (i.e., that the populations are significantly different in recombination rate, on the basis of phenotypic variance alone) than the Q_{ST} - F_{ST} analysis below.

QST-FST Analysis

To test the hypothesis that population-level differences in recombination rates are driven by natural selection, we performed a Q_{ST} - F_{ST} analysis [33, 35, 99]. We began by computing a point estimate of Q_{ST} for genome-wide recombination rate using Im4 by fitting a linear mixed effects model with the following form: $crossover\ count = intercept + (1|inbred\ line) + (1|population)$. We extracted the variance components for population and inbred line (nested in population) using the R function `varcomp()`. Following [55] we computed Q_{ST} using the following formula:

$$Q_{ST} = \frac{\sigma_{BG}^2}{\sigma_{BG}^2 + \sigma_{WG}^2}, \quad (\text{Equation 1})$$

where σ_{BG}^2 denotes the between-group (population) variance and σ_{WG}^2 denotes within-group (inbred line nested in population) variance. Note that the within-group variance term in the denominator is not multiplied by two in the case of haploids or completely inbred lines [99].

We computed F_{ST} using SNPs genotyped via RAD-seq in wild AZ and UT individuals. To do this, we converted the GATK VCF to a SNP table using `vcfR` and the `tidyverse` package in R (see analysis scripts). We then converted the resulting SNP table for manipulation in the R package `SNPRelate` [100]. Using `SNPRelate`, we first performed LD pruning (default settings, $r < 0.2$) to reduce statistical non-independence between SNPs [101]. This resulted in a dataset composed of 16 individuals for AZ and 42 for UT, with a total of 6 591 high quality SNPs. We then computed per-SNP estimates of Weir and Cockerham's F_{ST} using `SNPRelate`, requiring filtered sites to have a minimum minor allele frequency of 0.1.

We assessed the statistical departure from neutrality for each value of Q_{ST} using the Null-QST method outlined in [35] and [55] with a modification to accommodate trait data from inbred lines. The general approach outlined in these two references is to simulate the expected distribution of for a *neutral* trait (denoted Q_{ST}^n , neutral Q_{ST}) via a parametric bootstrap, and use this distribution as the basis of a statistical test of the hypothesis $Q_{ST} > Q_{ST}^n$.

To simulate the distribution of Q_{ST}^n we first estimated the between-group (σ_{BG}^2) and within-group (σ_{WG}^2) variance components. We obtained these values via REML estimation by fitting mixed-effects linear models using the function `lmer` in the R package `lme4` [98]. These models took the form $crossover\ count \sim intercept + (1|population) + (1|line)$. We extracted the variance components (standard deviations of the random effects) using the function `VarComp` from `lme4`.

We next generated 10 000 (nonparametric) bootstrap estimates of the mean value of Weir and Cockerham's F_{ST} by resampling the RADseq SNPs with replacement, and computing genome-wide mean F_{ST} using `SNPRelate`. We then generated 10 000 matching parametric bootstrap estimates of the σ_{WG}^2 by multiplying the REML point estimate by a random draw from a χ^2 distribution with degrees of freedom equal to the number of inbred families ($df = 17$). Next, we generated parametric bootstrap estimates of the expected values of σ_{BG}^2 for a neutrally evolving trait using the equation:

$$boot(\sigma_{BG}^2) = \frac{boot(F_{ST})boot(\sigma_{WG}^2)}{1 - boot(F_{ST})} \times \chi^2(n = 1, df = 1), \quad (\text{Equation 2})$$

with Equation 2 above being modified from [35] to accommodate complete inbreeding. In Equation 2, “boot” indicates individual bootstrap samples for each quantity, and the χ^2 term represents a draw from a χ^2 distribution with degrees of freedom equal to the number of populations minus one (one, in this case). This procedure results in 10 000 bootstrap samples for σ_{BG}^2 and σ_{WG}^2 , from which we computed 10 000 bootstrap samples of Q_{ST}^n using Equation 1. We finally computed a p value for the observed value of Q_{ST} by determining the number of Q_{ST}^n values that exceeded the observed value of Q_{ST} distribution. We also computed a confidence interval for $Q_{ST} - F_{ST}$ (the difference between Q_{ST} and F_{ST} , expected to be zero under the neutral model) by subtracting each value the $Q_{ST}^n - F_{ST}$ distribution from the observed value of $Q_{ST} - F_{ST}$ (after [55]). Note that while we computed the distribution of F_{ST} from the independently-sourced RAD-seq data, the distribution of F_{ST} was nearly identical when computed using SNPs derived from the short read whole genome sequencing of the inbred lines themselves.

Candidate genes associated with recombination differences

Using the candidate gene data from the inbred lines, we tested for associations between inbred line recombination estimates and genotype at each site where at least one non-synonymous change occurred in each gene. To this end, we fit linear models with recombination rate as the response and genotype (at all variable non-synonymous sites) as the predictor. This yielded a p value for each genotype versus recombination comparison. In order to control for the possibility of false positives, which we adjusted via the FDR approach [102], with FDR < 0.05 adjustments performed using the function `p.adjust` in R. A main caveat to this approach is that the small number of lines and large number of variable sites limits our power and ability to include controls for genetic background, genotype at “non-meiosis” genes, etc. As such, we consider the function of this analysis to be mainly hypothesis-generating and to serve as a bridge between our results in previous molecular work.

Association between local structural variation and recombination rate

We tested the association between normalized sequence homology and recombination rate via a hierarchical linear model fit using the function `glmer` from the R package `lme4` [98]. This model had the form: $recombination\ rate \sim method * homology + (1|window\ identity) + (1|inbred\ line)$, with Poisson-distributed errors and a log link function. Assigning window identity (i.e., genomic region in which recombination and homology were measured) as a random effect controls for mean local variation in recombination rate

(i.e., normalizes the absolute recombination rates among windows). Similarly, modeling inbred line identity as a random effect controls for genome-wide differences in recombination rate, which are unrelated to local variation. We assessed the significance of the homology term in the model by comparing the full model to a model with only random effects via a likelihood ratio test in R. We finally repeated this model fitting procedure with the normalized count of differences in structural variant alleles as the predictor.

DATA AND CODE AVAILABILITY

All analysis code employed throughout the paper is available as a Git repository at: https://github.com/ksamuk/samuk_et_al_curr_biol_2020. GT-seq amplicon data are available on Dryad <https://doi.org/10.5061/dryad.jsxksn062>. The accession number for the ddRAD data derived from wild populations is SRA: PRJNA610904. The accession number for the whole genome short read (HiSeq 4000) sequencing of the isolines is SRA: PRJNA610029. The accession number for the whole genome long read (PacBio Sequel) sequencing of the isolines is SRA: PRJNA610090.